Title
Molecular Characterization and Validation of Retinal Cell Types in the Sea Lamprey

Author
Pahlevan, Ali

Publication Date
2023

Peer reviewed|Thesis/dissertation

UNIVERSITY OF CALIFORNIA

Los Angeles

Molecular Characterization and Validation of Retinal Cell Types in the Sea Lamprey

A thesis submitted in partial satisfaction of the requirements for the degree Master of Science in Physiological Sciences

by

Ali Pahlevan

2023

ABSTRACT OF THE THESIS

Molecular Characterization and Validation of Retinal Cell Types in the Sea Lamprey

by

Ali Pahlevan

Master of Science in Physiological Science

University of California, Los Angeles, 2023

Professor Yi-Rong Peng, Co-Chair

Professor Gordon Fain, Co-Chair

Humans rely heavily on vision to navigate and perform complex tasks, making it a crucial sensory modality. However, the mechanisms underlying the emergence of this modality are not yet fully understood. Thus, understanding the origins of the visual system is a critical goal of neuroscience, as it can help define poorly understood neural circuitry. This project proposes a descriptive investigation to determine the molecular and evolutionary underpinnings of vision formation, specifically focusing on cell-type mapping and region-specific gene expression in basal vertebrate lamprey species. By localizing key regulatory genes and identifying the cell types of our vertebrate ancestors, we can elucidate the developmental processes and functional mechanisms of vision, ultimately providing an evolutionary roadmap of retinal vision. This

investigation significantly enhances the existing cellular taxonomy of retinal formation and reveals components of visual circuits that were prevalent even in the most primitive vertebrates.

The thesis of Ali Pahlevan is approved.

Kacie Deters

Gordon Fain, Committee Co-Chair

Yi-Rong Peng, Committee Co-Chair

University of California, Los Angeles

2023

TABLE OF CONTENTS

LIST OF FIGURES

ACKNOWLEDGEMENT

This project would not have been possible without the help of several individuals. I would like to express my deepest gratitude to my thesis advisor, Dr. Peng, for her support and guidance throughout the entire process. I would also like to thank the members of my thesis committee, Dr. Fain and Dr. Deters, for their time and valuable feedback on my work. I would like to extend my appreciation to Dr. Peng and Dr. Lin Zhang for contributing the bioinformatic elements of this project and for allowing me to collaborate on her paper. I would also like to thank my colleagues and friends for their encouragement throughout this journey. Finally, I would like to express my gratitude to my parents and sister for their unconditional love, support and patience throughout my academic journey. This thesis is a testament to their unwavering support and encouragement. Thank you all for your contributions to this work.

INTRODUCTION

Humans rely primarily on their sense of vision to navigate and perform complex tasks. In situations where our other senses such as smell or taste fail, our ability to see plays a crucial role in protecting us from our immediate environment[1]. Therefore, studying the visual system is a critical goal of neuroscience as its development, function, and connectivity help explain significant neural circuitry.

The process of vision[2] begins with light passing through the protective cornea and towards the lens. Supporting ciliary muscles then adjust the lens shape to refract and focus light onto a thin layer of retinal tissue in the posterior portion of the eye. At this location, the light photons undergo phototransduction, converting them into neural signals, which are then transmitted to the optic nerve. At the optic chiasm, the optic nerve crosses over and forms the optic tract, which carries visual information through the thalamus, specifically the lateral geniculate nucleus (LGN). Here, the information is processed and transmitted to the occipital lobe of the primary visual cortex for further interpretation.

In order to comprehend the organization and function of a complex structure such as the retina, it is essential to identify the cell classes and cell types that comprise it. Cell types are characterized based on their morphological and functional features, which include dendritic pattern, somatic position, axon innervation, and connection choice[3,4]. In the 19th century, Ramon y Cajal used Golgi staining to become the first scientist to create a comprehensive description of the neural cell-types in the retina[5]. However, cell-type classification lost popularity in the latter half of the 20th century as molecular and physiological methods advanced[6]. Projects with purely descriptive yield lost attention to hypothesis-driven research. Nevertheless, in the past decade,

cell-type categorization has been re-appreciated as a necessary requisite for understanding neural mechanisms. Building a complete taxonomy of retinal cell types enhances our comprehension of how healthy eyes operate and sheds insight into the mechanisms behind retinal pathology and retinal evolution.

The human retina comprises five neuronal classes, which are further classified into approximately one hundred cell types[7]. The cell bodies are arranged in three nuclear layers: the outer nuclear layer (ONL,) the inner nuclear layer (INL), and the ganglion cell layer (GCL); and two synaptic layers: the outer plexiform layers (OPL) and inner plexiform layers (IPL)[2,7,8] (Figure 1). Within the ONL, photoreceptors (PRs) convert a photon's kinetic energy into an electrochemical signal. At the OPL, rod and cone photoreceptors release excitatory glutamate onto the dendrites of bipolar cells (BCs) and horizontal (HCs)[9]. HCs laterally provide feedback and feedforward between PRs and BCs, and BCs project across the IPL to relay signals to retinal ganglion cells (RGCs) and amacrine cells (ACs). ACs secrete GABA or glycine across the IPL, providing inhibitory feedback and feedforward between RGCs and BCs. Finally, RGC axons converge and form the optic nerve, which transmits the retina’s visual information to areas of the primary visual cortex, where they are perceived as visual features such as color, motion, direction, form, and illumination[10,11].

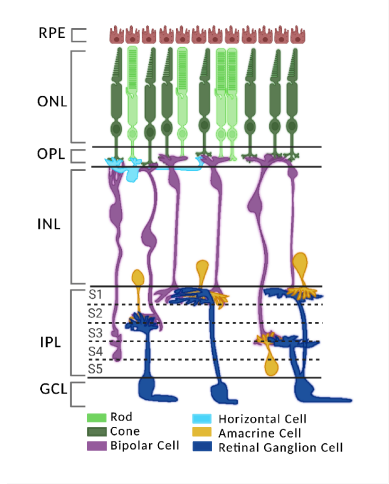

Figure 1. Sketch of peripheral primate retina showing its major cell classes and layers.

The retina's highly complex connectivity and laminar structure is truly astonishing, but the evolutionary mechanisms underlying its formation remains elusive. While primates and mice have been the primary model organisms for studying cell types in the visual system[12], it is crucial to shift our focus and create a cell-type atlas for our ancient phylogenetic ancestors. Doing so will help clarify both the developmental processes and functional mechanisms underlying the evolution of vision in vertebrate species.

The fossil record shows that the vertebrate lineage originated during the Cambrian explosion, a period of significant organismal diversification[13,14]. This ancestral lineage first gave rise to a superclass of jawless fish known as agnathans. Around 500 million years ago, a group of round-mouthed agnathans - referred to as cyclostomes - split off from the rest of the group and are recognized as the most ancient vertebrate species present in the modern day. Other agnathan lines later evolved to gnathostomes (jawed vertebrates), which gave rise to cartilaginous and ray-finned fishes, amphibians, reptiles, birds, and mammals (Figure 2). Currently, there are only two classes of cyclostomes still extant: the eel-like aquatic hagfish and lampreys, which together

make up 120 species. Among these is the sea lamprey, *Petromyzon marinus*, which represents the oldest living vertebrate species and offers a valuable tool for studying the evolutionary processes underlying the development of the visual system in modern vertebrates. As an outgroup, it provides a unique perspective on the early stages of vertebrate evolution and sheds light on the genetic and molecular mechanisms that have contributed to the diversity of visual systems in vertebrates today.

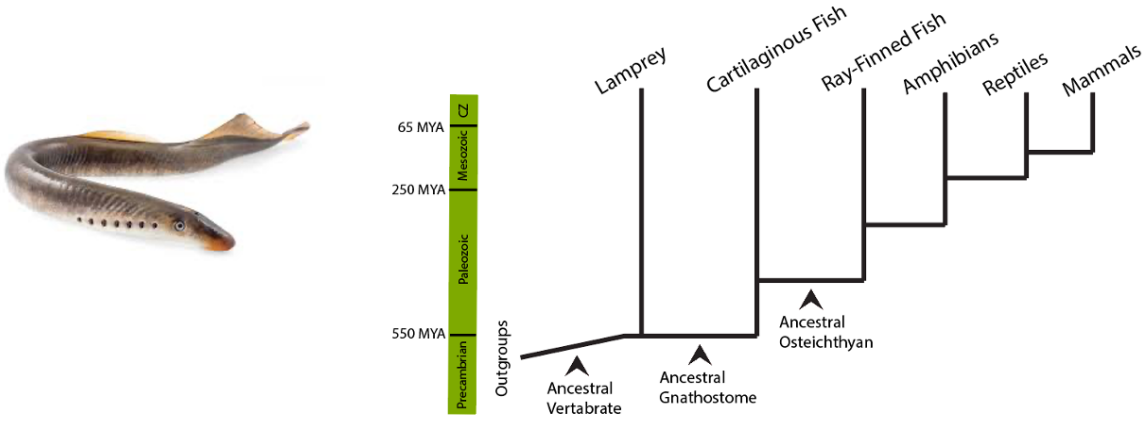

Figure 2. Lamprey sit at the evolutionary node between invertebrates and vertebrates. They are amongst the most ancient vertebrate species present in the modern day.

Morphologically, lamprey possess a laminated retina composed of the INL, ONL, and GCL with the major cell classes: PRs, BCs, HCs, ACs, RGCs, and MG[4,15]. Gnathostomes typically display differing morphologies in the outer segments of rods and cones[4]. In modern mammals, PR disks of rods are separated and pinched off from the plasma membrane, whereas the membrane lamellae of cones are continuous with the plasma membrane[2]. In lamprey,

however, the structure of the outer segments of the two PRs, “short” PRs and “long” PRs, is identical and generally resembles the structure of a mammalian cone[4,15]. Based on this observation, it was suggested that the "short" PRs may not be genuine rods and that both the "short" and "long" PRs could potentially be two distinct types of cones. However, electrophysiological assays have demonstrated that the lampreys' "short" and "long" PRs exhibit light adaptation, photobleaching, and response kinetics to flashes of light comparable to rods and cones[4,16]. Histological studies have also found the presence of PDE6 proteins, transducins, and cGMP-gated cation channels in lamprey PRs[17,18]. These findings suggest that our ancient vertebrate ancestors relied on a functionally similar phototransduction cascade to that in modern vertebrates. This high frequency of shared derived (i.e. synapomorphic) constituents of the transduction cascade indicates that this is unlikely to have been the result of convergent evolution, suggesting that the fundamental properties of rod and cone emerged very early and that the evolution of rods from cones must have happened early in vertebrate evolution[4,14]. The ancient emergence of these fundamental properties likely evolved to meet environmental requirements and became phylogenetically determined within early vertebrate species.

While many retinal features appear to have converged, particularly in the ONL, there are several noteworthy differences in the laminar organization of the lamprey retina**,** particularly in the inner layers**.** In gnathostomes, RGC axons run along the vitreal side of the retina, deep in the RGC layer near the inner limiting membrane[19]. However, in lamprey, there is an optic fiber layer (OFL) situated between the INL and IPL[20]; a unique organization not observed in any gnathostome species (Figure 3). Furthermore, adult lamprey have distinct RGC types in their INL, which differ from known gnathostome RGCs. Unlike in gnathostomes where RGC bodies

predominantly reside in the vitread RGC layer located in the IPL, only 40% of all lamprey RGCs localize in this area. Lamprey RGCs are instead distributed into inner and outer groups in the INL and IPL, further divided into the outer IPLo and inner IPLi[4]. Electron microscopy studies have also revealed that *P. marinus* has lower overall RGC densities compared to mammalian vertebrates[20]**.** Moreover, current lamprey literature presents six morphological RGC types (IGCa, IGCb, OGCa,OGCb, BPGCs, and OGCs). IGCa, IGCb, OGCa, OGCb are homologous to other vertebrate RGCs – with dendrites dispersed in the image-forming IPL and projecting to the tectum where they direct movements of the body, head, and eyes[20]. BPGCs and OGCs were not previously described in other adult vertebrates and distribute their dendrites to the OPL, contacting directly with PRs for rapid transduction of visual information. These two unique subtypes ultimately project to the pretectum, a midbrain nuclei region, controlling the dorsal light and visual escape responses[20].

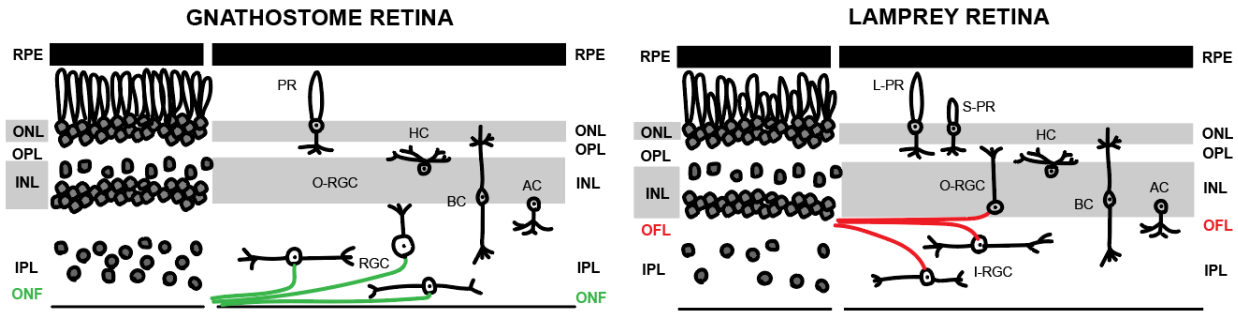

Figure 3. The ganglion cell axons come together within the optic fiber layer (OFL), situated between the INL and IPL, with ganglion cell bodies flanking both sides of the OFL.

Ramon y Cajal's morphological classifications revealed striking similarities between retinal circuits across different vertebrate species. These findings have been reproduced with

more advanced structural methods in recent years[7,21,21]. For instance, comparative single-cell analysis has shown a high degree of conservation of interneuron types between mice and macaques[7]. However, this study found that conservation was stronger for cell types located closer to outer retinal layers. In other words, cell types in the outer layer (e.g. PRs, HCs) are transcriptomicaly more similar between these two species than the corresponding cell types in the inner layers (e.g. RGCs). The unique arrangement of RGCs in the lamprey retina further supports the notion that there is a lower level of convergence among cell types in the lower retinal layers. Although research has been done to investigate lamprey PRs and RGCs, few projects have explored the conservation for other retinal cell types such as HCs, BPs, and ACs. Moreover, despite our extensive knowledge about gene conservation and evolution, our understanding of the evolution and conservation of retinal cell types remains limited[21].

The techniques used to study different cell types in the lamprey retina have been mostly rudimentary, relying on immunohistochemistry (IHC) and electron microscopy. Despite nearly 50 years of research using IHC, only a few reliable markers have been identified to target specific cell types in the lamprey retina. For example, anti-Pγ2 have been demonstrated to select long photoreceptors, while anti-Pγ1 has specifically marked short PRs[4,23,24,]. However, specifically targeting other cell types has been challenging, as studies have yielded conflicting results. For instance, calretinin – a known canonical marker for RGCs – has inconsistently been localized in a combination of BCs, HCs, and ACs using IHC in different experiments[25,26,27]. Similarly, studies using IHC have reported conflicting results regarding the presence of the calcium binding protein calbindin in lamprey RGCs[26,27]. It is evident that the existing tools known to label cell types in mammals are not effective for identifying cell types in lampreys.

Recent breakthroughs in single-cell transcriptomic technology have led to the creation of retinal cell-type atlases for a variety of vertebrate species, including humans, macaques, chickens, mice, and zebrafish[7,28]. These studies suggest a conserved retinal plan across modern vertebrates that is similar in composition and structure to humans, with some differences in the proportions and number of subtypes. In the current study, we present a novel single-cell atlas for the adult lamprey retina. Specifically, we conducted histology and fluorescent in situ hybridization (FISH) to precisely localize and validate single-cell RNA sequencing – ultimately uncovering synapomorphic and unique retinal features between lamprey and modern vertebrates. Our goal was to identify potential biomarker labels for lamprey retinal cell types, including rods, cones, ON and OFF starburst ACs, HCs, BP cells, RGCs, and intrinsically photosensitive RGC (ipRGC). By identifying a systematic categorization of lamprey retinal cell-types, we hope to enhance our evolutionary understanding of the vertebrate retina, thus providing insight into visual processing circuits.

MATERIALS AND METHODS

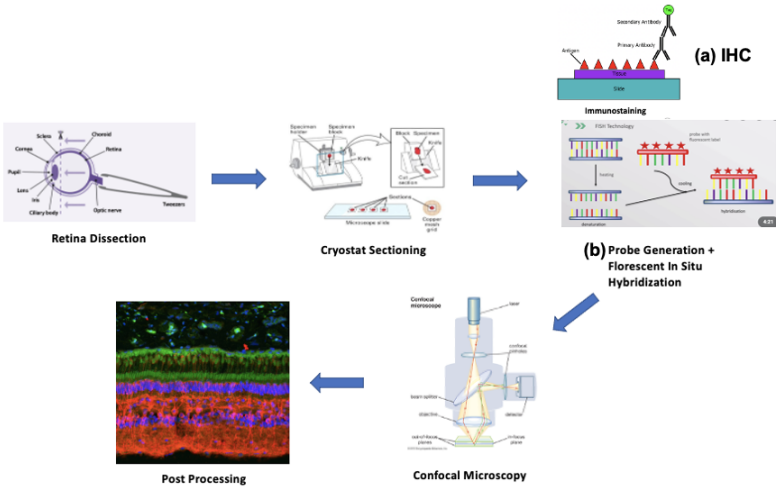

Figure 4. Brief overview of the sample preparation and processing protocol.

Lamprey Tissue

The animal experiments conducted in this study followed the NIH guidelines and were approved by the Institutional Animal Care and Use Committee (IACUC) at the University of California, Los Angeles. Post-mortem collection of adult Lamprey eyes was performed for the histological and in situ studies. The eyes were transported immediately to the lab in a humidity chamber and subsequently fixed in 4% paraformaldehyde/PBS for 60-90 minutes on ice.

Retinal Dissection

The lamprey retina was fixed and then dissected under a dissection microscope with the anterior structures and lens carefully removed. The dissected retinal tissue was then transferred to a solution of 30% sucrose and 0.2% azide until the tissue sank, which typically took upwards of 2 hours at 4°C. The retinal tissue was embedded in O.C.T. medium and frozen in a 2-methyl butane solvent on dry ice at -80°C. The resulting block was stored at -80°C until cryostat sectioning.

Sectioning

The retinal tissue was sectioned into 20 μm thickness with a cryostat and subsequently mounted on slides. The sections were stored at -80°C for future use.

Immunohistochemistry (IHC)

Frozen slides were thawing for 30 minutes at room temperature (RT). The sections were then rehydrated in 1X PBS three times for 5 minutes (3 x 5 minutes) each. Slides were placed in a moisture chamber and 300 μL of a 5% serum + 0.3% Triton X-100 in PBS was added to the inside of the PAP ring to reduce the chance of nonspecific binding. After 1 hour, the blocking solution was replaced with a 300 μL mixture of (1:300, 1:500, or 1:1000) primary antibody (Ab) + 3% donkey serum + 0.3% triton, and left at 4°C in a humidity chamber overnight. After the primary Ab was removed, sections were washed with 1X PBS (3 x 5 minutes). Next, secondary Ab (1:1000) + 3% donkey serum + 0.3% triton mixture was pipetted onto slides and left to incubate at RT for 90 minutes. The secondary Ab conjugated to a fluorophore was raised against the species in which the primary Ab was made. Then, 200 μL of the secondary Ab mixture was removed and mixed with DAPI (1:1000). The DAPI mixture was pipetted back onto the slide and left to incubate at RT for an additional 30 minutes. The section was washed for a third and final time in 1X PBS (3 x 5 minutes). After the slide was completely dried, a glass coverslip was placed onto the slide and bound with 20 μL of a mounting solution. Finally, the edges of the cover slip were sealed with ethyl acetate.

RNA Probe Synthesis for FISH

RNA was extracted from dissected retinas with the RNAeasy kit[29]. We performed UV spectrophotometry with the NanoDrop instrument to determine the concentration of the extracted

RNA, and to ensure purity from proteins and salts. A cDNA library was then synthesized with the Azura 1996 RT PCR protocol[31]. Using gene sequence numbers from the single-cell annotation, we generated forward and reverse primers of interest with the NCBI nucleotide database browser and NCBI Primer-BLAST. We added a T7 promoter sequence to the reverse primer to facilitate in vitro transcription in the later RNA probe synthesis steps. Phusion PCR (PCR1) was conducted with transcript specific primers, followed by cleanup with the Qiagen PCR cleanup kit[32] to remove contaminants and impurities that could interfere with downstream analysis. We performed another NanoDrop to confirm the purity and concentration of the PCR product after cleanup. In vitro transcription (PCR2) was then carried out in an RNAse free environment with T7 RNA polymerase and nucleotide labeling mix. An RNAse free environment was maintained from this point on until the second day of the in situ protocol to prevent RNA degradation. To ensure size and quality, we ran the RNA probes on a 1% agarose gel. Any remaining DNA was digested by Roche DNAse before precipitating the RNA probes to be used in the in situ protocol.

Fluorescence In Situ Hybridization (FISH)

Sample preparation: frozen retina sections were thawed at RT for 30 minutes and then incubated at 65°C for an additional 30-60 minutes to prepare for hybridization. The slides were fixed for 10 minutes in 4% PFA in coplin jars, followed by washing with 1X PBT (3 x 5 minutes). The slides were then washed with Proteinase K Solution for 5 minutes, followed by another round of washing with 4% PFA (2 x 5 minutes) and 1X PBT (3 x 5 minutes). Acetylation solution was applied to the slides to contribute to polymerization, followed by washing with 1X PBS (3 x 5 minutes) before air drying at RT. Hybridization: The slides were placed in a humidified slide box

with paper towels soaked in pre-hybridization chamber solution, and then 200 µL of pre-hybridization solution (pre-warmed to 65°C) was applied and incubated for one hour at 65°C. DIG-labeled, Fluo-labeled, or DNP-labeled RNA probes were added to hybridization solution on ice, and then added to pre-warmed hybridization solution. The probes were added to the slides, coverslipped, and incubated overnight at 65°C. On the second day of the in situ protocol, post-hybridization washes were performed with different concentrations of SSC wash solutions pre-warmed to 65ºC. The slides were washed in a 50:50 solution of 2X SSC and pre-hybridization solution at 65ºC (2 x 30 minutes). The slides were then washed with 2X SSC at 65ºC (2 x 30 minutes), followed by additional washes with 0.2X SSC (2 x 30 minutes) at 65ºC. Next, the slides were washed in MABT (3 x 5 minutes) at RT, with the last wash being on the slides. The slides were then blocked in HISS/MABT/blocking solution for an hour at RT. Antibody incubation was performed by adding α-DIG-HRP to HISS/MABT/blocking solution (1:1000) and then adding 200 µl/slide. The slides were then incubated overnight at 4ºC in a humidified chamber with paper towels soaked in HISS/MABT. On the third day of the in situ protocol, slides were first washed with MABT for (6 x 5 minutes) at RT, followed by washes with PBT (3 x 5 minutes) on the slides. To prepare for TSA Amplification, slides were washed with TSA amplification diluent for 5 minutes, and then incubated in a tyramide working solution for 15-30 minutes. After incubation, the slides were rinsed 8 or more times with PBT on slides, and fluorescence was checked under the Echo Revolve fluorescence scope. If the fluorescence was not well developed, the slides were incubated with recycled tyramide working solution for an additional 10-20 minutes. HRP was inactivated by treating with freshly prepared 3.0% H2O2/PBT for 30 minutes on slides. After 3 washes with PBT and 6 washes with MABT on

slides, the slides were blocked in HISS/MABT/blocking solution for 1 hour at RT. If applicable, antibodies (α-DNP-POD or α-Fluorescein-POD) were added (1:500) to HISS/MABT/blocking solution, and then the slides were incubated overnight at 4°C in a humidified chamber with paper towels soaked in HISS/MABT. If the slides were stained with two probes, a fourth day was added to the protocol for another round of tyramide working solution. DAPI was stained for 20 minutes to localize cell nuclei, before washing the slides for the final time and mounting them with a coverslip.

Image Acquisition and Processing

Images were acquired with an Olympus FluoView FV1000 upright confocal microscope with 405, 488, 514, 559, 647 lasers. The images were acquired with 40X and 60X oil lenses, with a resolution of 1,024 x 1,024 pixels and a step size of 1μm. Images were processed and analyzed with the Fiji ImageJ software to generate maximum intensity Z-projections. Adobe Photoshop was used for adjustments to brightness and contrast. Adobe Illustrator was used to organize and generate the figures.

Single Cell RNA Sequencing and Analysis

To generate single-cell suspensions, our lab utilized the papain dissociation system. Subsequently, the Chromium 10X Genomics scRNA-seq protocol was followed to profile gene expression at an unbiased single-cell level, and to gain a comprehensive understanding of cellular heterogeneity within the lamprey retinal tissue. Specifically, this protocol employs a droplet-based microfluidics technique, which allows for targeting and individual barcoding of cells through the application of pressure to the cell suspension. The cells are then passed through tiny tubes one-by-one, which enables their isolation in an oil droplet along with a unique barcode

that tags each individual cell. The mRNAs are then amplified with PCR. Using this amplification, Dr. Peng generated unique molecular identifier count matrices with CellRanger analysis. Finally, she conducted dimensionality reduction and clustered these count matrices based on transcriptional similarities with the Seurat pipeline in R.

RESULTS

A novel atlas of lamprey retinal cell types was generated based on transcriptional similarities, identifying 54 distinct retinal cell types among 22,000 retinal cells. To visualize the data, a heat map of the six major cell classes was created from known canonical markers (Figure 5). Since the accuracy of the analysis relies heavily on annotation, the analysis was paired with protein and mRNA localization techniques for validation and increased confidence in the results.

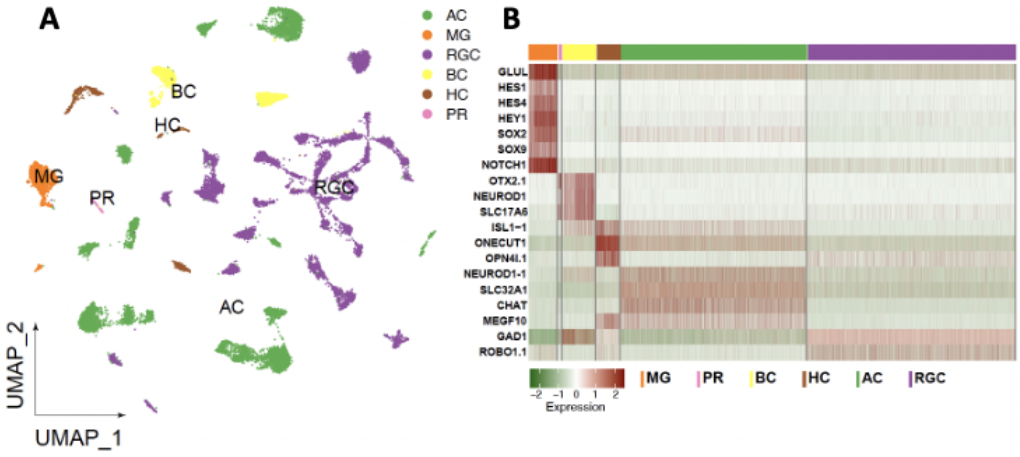

Figure 5. (A) UMAP visualization of the 54 identified cell types clustered into 6 distinct cell classes. (B) Heatmap showing canonical marker genes for each of the cell classes.

IHC

The IHC validations were in line with prior lamprey IHC studies, which showed that antibodies known to label cell types in mammals were not consistently effective for identifying cell types in lamprey. For example, weak nonspecific signals for GNTG1, a marker that should have been highly specific for rods, were observed (Figure 6A). 7G6, OPN1SW, and Isl1 stainings followed similar nonspecific patterns against their respective cell types. In other instances, antibodies mislabeled incorrect cell types, such as VGLUT3, which is a specific marker for glutamate

releasing ACs (Figure 6B). Based on the annotation, its expression was expected in this lamprey cell type, but the antibody staining clearly mislocalized in the photoreceptor layer. In the case of rhodopsin and PRKCA, the antibodies accurately labeled cell types corresponding to the single-cell annotation observed for other vertebrates (Figure 6C-D). In other words, the presence of photoreceptor and bipolar cell classes were initially validated through IHC. Nevertheless, the consistency and accuracy of IHC were too insufficient to be reliable for the remaining cell-class validations. Therefore, a more advanced molecular technique was used for the remainder of the study.

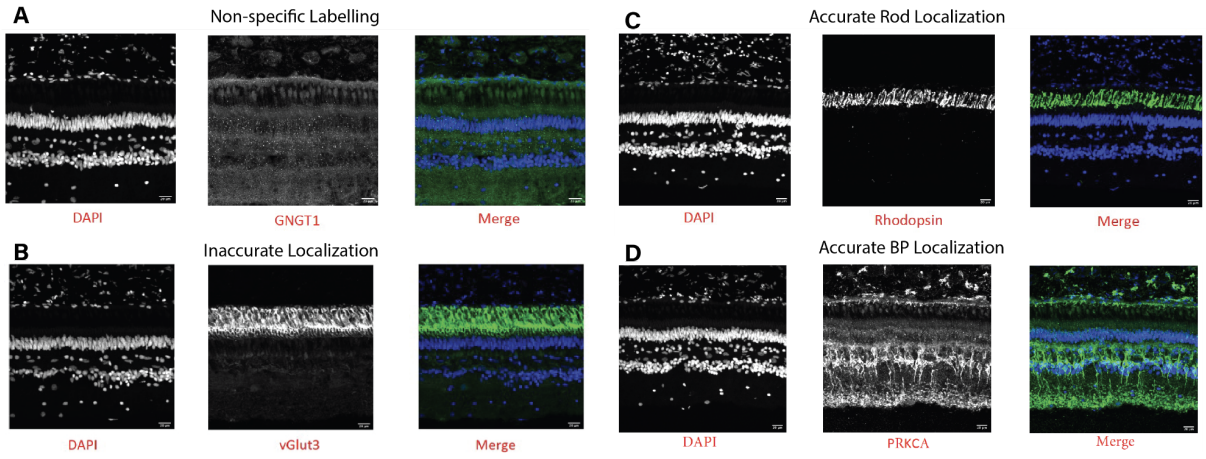

Figure 6. Unreliable validation from IHC. (A) Weak non-specific localization of GNGT1 and (B) inaccurate localization of vGlut3. (C-D) Accurate localization of Rhodopsin and PRKCA in rods and bipolar cells, respectively.

FISH

Due to IHC limitations, FISH was used in the remainder of the study to validate the cell-class annotation. SLC32A1, which codes for a vesicular inhibitory amino acid transporter, and NEUROD1 were found in the AC clusters (Figure 5B). In situ validated the presence of these

transcripts in the AC cluster (Figure 7). Additionally, a subset of NEUROD1 was expressed in a group of BP cells located further out in the INL, consistent with the annotation.

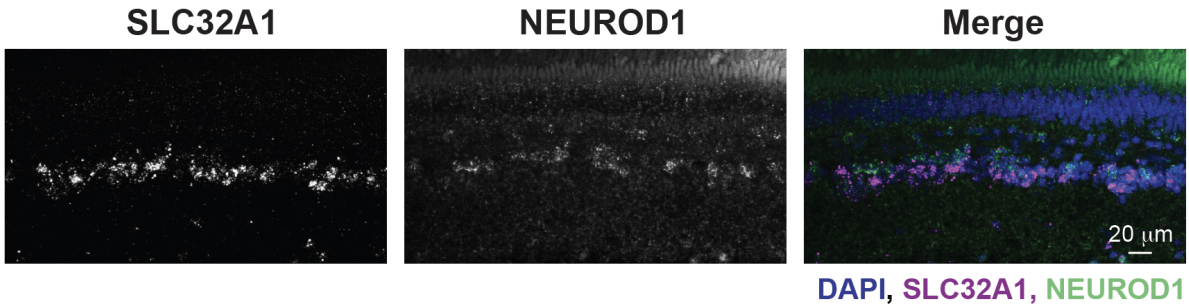

Figure 7. SLC32A and NEUROD1 localized in the AC cells. NEUROD1 was also found in a subset of BP cells.

OPN4, melanopsin, was annotated in the RGC cluster. One isoform of OPN4, OPN4l.1, was found with in situ in a subset of horizontal cells, as well as RGCs that were localized higher up in the INL. IHC localized OPN4 near a subset of L-cones distinct from rods in the PR layer (Figure *8*).

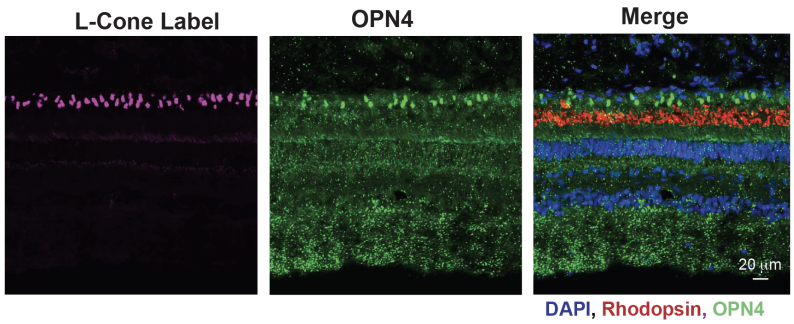

Figure 8. OPN4 localized near a subset of L-Cones distinct from rods via IHC. OPN4l.1 found in a cluster of HCs and RGCs with in situ (not pictured).

In total, the RGC cluster was composed of 26 RGC types. Interestingly, we observed the expression of GAD1 or Glutamate decarboxylase 1 in RGCs, despite it being typically considered as an amacrine cell marker. Moreover, SLC17A6, which is a known global marker for all RGCs, was only localized in a subset of RGCs (Figure 9).

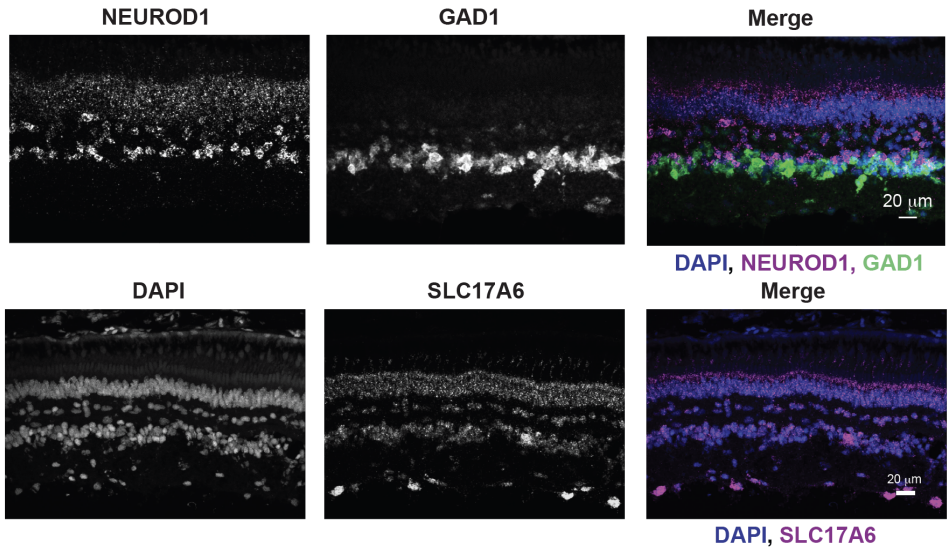

Figure 9. Unique expression of GAD1 and SLC17A6 in lamprey RGC types.

Within the PR cluster, two subclusters, labeled L-PR and S-PR, were identified - shown by UMAP analysis (Figure 10A). The differential gene expression between these two subclusters is depicted through dotplot analysis (Figure 10B). In situ validations confirmed the presence of these distinct PR subclasses (Figure 10 C-D), consistent with the IHC results. Rhodopsin, coded by the RHO gene, was detected in the outer segment of the photoreceptor and co-stained with transducinS, suggesting that the short photoreceptor is rod-like. Similarly, red-opsin, which codes for red-sensitive opsins, was co-stained with transducinL, indicating the presence of long cone-like photoreceptors. Additionally, GLUL expression was observed around the majority of

cell classes and localized across different layers, indicating its glial role in supporting all other cell classes.

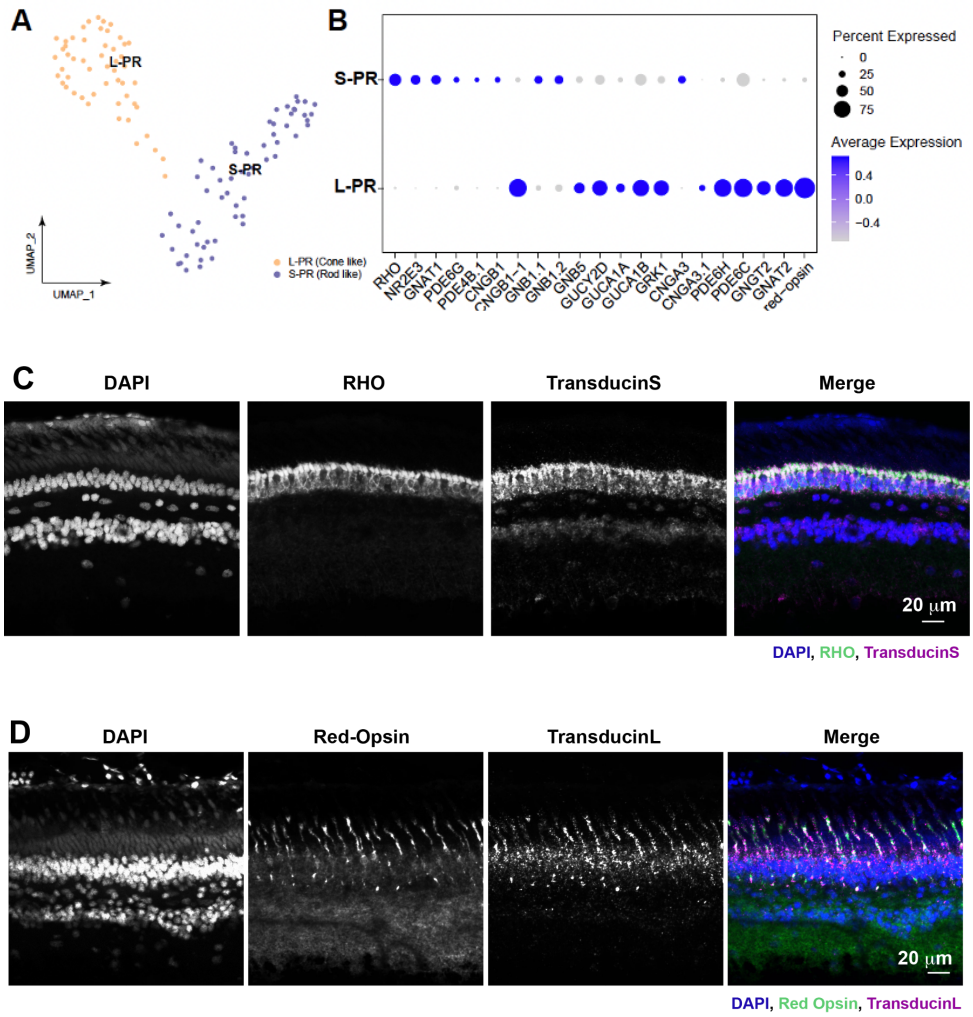

Figure 10. Lamprey exhibit distinct S-PR and L-PR clusters. (A) UMAP of the PR cluster demonstrates two PR types. (B) Dotplot displays differential gene expression between S-PR and L-PR. (C) In situ validation of S-PR and (D) L-PR.

We performed a detailed analysis on a subset of ACs, which revealed the presence of starburst ACs. We validated the presence of this subclass from known markers such as CHAT (Choline

acetyltransferase) and the MEGF10 transmembrane protein transcript (Figure 11). Furthermore, the FEZF1 gene, which is known to be a transcriptional switch that determines the fate of ON amacrine cells, was absent in lamprey. However, sequencing revealed the presence of another protein in the FEZF family, FEZF2.

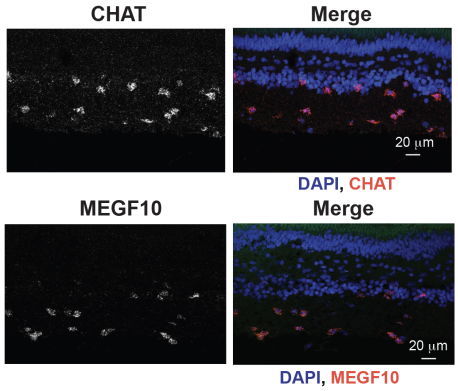

Figure 11. In Situ validation indicates the presence of ON and OFF starburst AC cells expressing CHAT and MEGF10 in the GCL and INL of the lamprey retina.

DISCUSSION

A novel atlas of lamprey retinal cell types was created by the use of a transcriptomic approach, revealing 6 conserved cell classes consisting of 54 distinct cell-types. While the major cell classes are conserved, the transcriptomic identities vary in terms of their level of conservation. Validation of this analysis from imaging techniques revealed unique features in lamprey retinas. The results indicated that the PR, BP, AC, HC, RGC, and MG classes were already specified during the early evolution of vertebrates. Therefore, the similarities observed between the retinas of contemporary vertebrates and cyclostomes are likely due to ancient features that existed in the ancestral vertebrate. Based on the consistent laminar structure of the retina in gnathostomes, it is unlikely that these similarities evolved through convergent evolution.

The IHC validations were consistent with prior studies of lamprey IHC, indicating that antibodies commonly used to label cell types in mammals are not always effective for identifying cell types in lamprey. However, we have identified a list of reliable antibodies that can be used in further experiments for validation purposes. Furthermore, our in situ experiments have provided a comprehensive list of effective and ineffective primer pairs that can be utilized for creating fluorescent RNA probes in future in situ studies.

Overall, our approach provides insights into some interesting retinal features. IHC labeling of OPN4 indicated the presence of melanopsin proteins in photoreceptor layers. In humans, melanopsin is found in approximately two percent of RGCs, specifically the ipRGCs, which respond to blue light wavelengths and do not rely on interneurons in their signaling pathway[33]. It is possible that our IHC staining labeled the dendrites of these unique RGCs in the PR layer. Additionally, single-cell annotations and in situ validations showed that OPN4L.1 was found in a subset of RGCs located higher up in the INL, supporting the presence of outer RGC

types in ancient vertebrates. The non-image-forming visual functions of ipRGCs, such as the activation of the circadian rhythm, hormone secretion, and control of the pupillary light reflex[34,35], suggest lower levels of parallel processing, which may explain why this cell type does not require information processing performed by other interneurons.

We have expanded our knowledge and identified a more accurate quantity of RGC types to 26, compared to the previously defined six morphological types. We also observed unique gene expression patterns within the RGC cluster. For example, we found expression of GAD1, which is typically a marker for amacrine cells in gnathostomes, in RGCs. Furthermore, we observed that SLC17A6, a global marker for all RGCs in humans, was only localized to a subset of lamprey RGCs.

We also discovered that although the morphology of lamprey PRs is inconsistent with modern vertebrates, the expression patterns of short PRs and long PRs indicate that they are rod-like and cone-like, respectively. This finding suggests that the functional evolution of rods from cones must have occurred during the evolution of vertebrates. Additionally, we identified that transducinS and transducinL are unique to the lamprey species, and these prototypic G-proteins most have likely later evolved and converged into the single transducin gene involved in the phototransduction pathways of modern vertebrates

A detailed analysis of a subset of amacrine cells revealed the presence of starburst amacrine cells in our vertebrate ancestors. These findings were validated by markers such as CHAT and MEGF10. In modern vertebrates, there are two types of starburst amacrine cells, the ON and OFF types, which reside in the GCL and INL, respectively. Key marker expressions in both these layers in lamprey suggest that ON and OFF starburst amacrine cells were present when vertebrates first evolved. Furthermore, the presence of the transcriptional switch for ON

amacrine cells, FEZF2, in nearly half of all starburst amacrine cells indicates the early emergence of ON amacrine cells.

CONCLUSION

The relatively minor differences in gene expression between lamprey and modern vertebrates can be attributed to the independent evolutionary demands and processes that occurred in gnathostomes and cyclostomes. Despite this, it is impressive how much the retinal structure has been conserved over the past 500 million years. The precise laminar organization of the retina that emerged early in vertebrate evolution provided our ancestors with an adaptive advantage in their environment. Lamprey present a unique opportunity to study ancient visual system features and gain further insights into the evolution of the vertebrate retina. Our study provides a molecular foundation for future studies devoted to exploring the retinal cell-type features in this species.

References

1. Dominy, Nathaniel, et al. "Ecological Importance of Trichromatic Vision to Primates." *Nature*, vol. 410, no. 6826, 2001, pp. 363–366.
2. Armstrong, R. A., and R. P. Cubbidge. "The Eye and Vision: An Overview." *Handbook of Nutrition, Diet and the Eye*, Academic Press, 15 Apr. 2014.
3. Kim, Ungsoo Samuel et al. "Retinal Ganglion Cells-Diversity of Cell Types and Clinical Relevance." *Frontiers in neurology* vol. 12 661938. 21 May. 2021, doi:10.3389/fneur.2021.661938
4. Fain, Gordon L. "Lamprey vision: Photoreceptors and organization of the retina." *Seminars in cell & developmental biology* vol. 106 (2020): 5-11. doi:10.1016/j.semcdb.2019.10.008
5. Garcia-Lopez, Pablo, et al. "The Histological Slides and Drawings of Cajal." *Frontiers in Neuroanatomy*, Frontiers Research Foundation, 10 Mar. 2010.
6. Sanes, Joshua R., and Richard H. Masland. "The Types of Retinal Ganglion Cells: Current Status and Implications for Neuronal Classification." *Annual Review of Neuroscience*, vol. 38, no. 1, 2015, pp. 221–246.
7. Peng, Yi-Rong et al. "Molecular Classification and Comparative Taxonomics of Foveal and Peripheral Cells in Primate Retina." *Cell* vol. 176,5 (2019): 1222-1237.e22. doi:10.1016/j.cell.2019.01.004
8. Zhang, R et al. "Fine structure of the human retina defined by confocal microscopic immunohistochemistry." *British journal of biomedical science* vol. 78,1 (2021): 28-34. doi:10.1080/09674845.2020.1776586

9. Baden, Tom et al. “Understanding the retinal basis of vision across species.” *Nature reviews. Neuroscience* vol. 21,1 (2020): 5-20. doi:10.1038/s41583-019-0242-1
10. Gollisch, Tim, and Markus Meister. “Eye Smarter than Scientists Believed: Neural Computations in Circuits of the Retina.” *Neuron*, U.S. National Library of Medicine, 28 Jan. 2010.
11. Sanes, Joshua R, and S Lawrence Zipursky. “Design principles of insect and vertebrate visual systems.” *Neuron* vol. 66,1 (2010): 15-36. doi:10.1016/j.neuron.2010.01.018
12. Gordon, Joshua A., and Michael P. Stryker. “Experience-Dependent Plasticity of Binocular Responses in the Primary Visual Cortex of the Mouse.” *The Journal of Neuroscience*, vol. 16, no. 10, 1996, pp. 3274–3286., doi:10.1523/jneurosci.16-10-03274.1996.
13. Feinberg, Todd E, and Jon Mallatt. “The evolutionary and genetic origins of consciousness in the Cambrian Period over 500 million years ago.” *Frontiers in psychology*vol. 4 667. 4 Oct. 2013, doi:10.3389/fpsyg.2013.00667
14. Green, Stephen A., et al. “The Lamprey: A Jawless Vertebrate Model System for Examining Origin of the Neural Crest and Other Vertebrate Traits.” *Differentiation*, vol. 87, no. 1-2, 2014, pp. 44–51.
15. Govardovskii, Victor et al. “Visual cells and visual pigments of the river lamprey revisited.” *Journal of comparative physiology. A, Neuroethology, sensory, neural, and behavioral physiology* vol. 206,1 (2020): 71-84. doi:10.1007/s00359-019-01395-5

16. Morshedian, Ala, and Gordon L Fain. “Single-photon sensitivity of lamprey rods with cone-like outer segments.” *Current biology : CB* vol. 25,4 (2015): 484-7. doi:10.1016/j.cub.2014.12.031

17. Lamb, Trevor D et al. “Evolution of Vertebrate Phototransduction: Cascade Activation.” *Molecular biology and evolution* vol. 33,8 (2016): 2064-87. doi:10.1093/molbev/msw095

18. Muradov, Hakim et al. “Unique transducins expressed in long and short photoreceptors of lamprey Petromyzon marinus.” *Vision research*vol. 48,21 (2008): 2302-8. doi:10.1016/j.visres.2008.07.006

19. Bao ZZ. Intraretinal projection of retinal ganglion cell axons as a model system for studying axon navigation. Brain Res. 2008 Feb 4;1192:165-77. doi: 10.1016/j.brainres.2007.01.116. Epub 2007 Feb 2. PMID: 17320832; PMCID: PMC2267003.

20. Jones, Marcus Robert et al. “Selective projection patterns from subtypes of retinal ganglion cells to tectum and pretectum: distribution and relation to behavior.” *The Journal of comparative neurology* vol. 517,3 (2009): 257-75. doi:10.1002/cne.22203

21. Zeng, Hongkui, and Joshua R. Sanes. “Neuronal Cell-Type Classification: Challenges, Opportunities and the Path Forward.” *Nature Reviews Neuroscience*, vol. 18, no. 9, 2017, pp. 530–546.

22. Sanes, Joshua R., and S. Lawrence Zipursky. “Design Principles of Insect and Vertebrate Visual Systems.” *Neuron*, vol. 66, no. 1, 2010, pp. 15–36., doi:10.1016/j.neuron.2010.01.018.

23. Negishi, K., et al. “Two Types of Lamprey Retina Photoreceptors Immunoreactive to Rod- or Cone-Specific Antibodies.” *Vision Research*, vol. 27, no. 8, 1987, pp. 1237–1241.

24. Hoque, Ferdousi Arjana et al. “Immunohistochemical Characterization of the Development of Long Photoreceptor Cells in the Lamprey Retina.” *Zoological science* vol. 38,4 (2021): 326-331. doi:10.2108/zs200151

25. Villar-Cerviño, Verona et al. “Presence of glutamate, glycine, and gamma-aminobutyric acid in the retina of the larval sea lamprey: comparative immunohistochemical study of classical neurotransmitters in larval and postmetamorphic retinas.” *The Journal of comparative neurology* vol. 499,5 (2006): 810-27. doi:10.1002/cne.21136

26. Villar-Cheda, Begoña et al. “Calbindin and calretinin immunoreactivity in the retina of adult and larval sea lamprey.” *Brain research*vol. 1068,1 (2006): 118-30. doi:10.1016/j.brainres.2005.11.014

27. Dalil-Thiney, N et al. “Immunohistochemical localization of calbindin-D28K and calretinin in the lamprey retina.” *The Journal of comparative neurology* vol. 340,1 (1994): 140-7. doi:10.1002/cne.903400110

28. Yamagata, Masahito et al. “A cell atlas of the chick retina based on single-cell transcriptomics.” *eLife* vol. 10 e63907. 4 Jan. 2021, doi:10.7554/eLife.63907

29. “RNeasy Kits.” *QIAGEN*, https://www.qiagen.com/us/products/discovery-and-translational-research/dna-rna-purification/rna-purification/total-rna/rneasy-kits.

30. “Qiashredder.” *QIAGEN*, https://www.qiagen.com/us/products/instruments-and-automation/accessories/qiashredde.
31. “Azuraquant™ Cdna Synthesis Kit.” *AzuraQuant CDNA Synthesis Kit | Azura Genomics*, https://www.azuragenomics.com/azuraquant-trade-cdna-synthesis-kit.html.
32. “QIAquick PCR Purification Kit.” *QIAGEN*, https://www.qiagen.com/us/products/discovery-and-translational-research/dna-rna-purification/dna-purification/dna-clean-up/qiaquick-pcr-purification-kit.
33. Do, Michael Tri Hoang, and King-Wai Yau. “Intrinsically photosensitive retinal ganglion cells.” *Physiological reviews* vol. 90,4 (2010): 1547-81. doi:10.1152/physrev.00013.2010
34. Hu, Caiping et al. “Intrinsic physiological properties of the five types of mouse ganglion-cell photoreceptors.” *Journal of neurophysiology* vol. 109,7 (2013): 1876-89. doi:10.1152/jn.00579.2012
35. Morshedian, Ala et al. “Pupillary light reflex of lamprey Petromyzon marinus.” *Current biology : CB*vol. 31,2 (2021): R65-R66. doi:10.1016/j.cub.2020.11.021